Article

A new species in the spider family Myrmecicultoridae (Arachnida, Araneae) and evidence of myrmecophagy in the family

PAULA E. CUSHING[1*] & EDMUNDO GONZÁLEZ SANTILLÁN[2]

[1]*Denver Museum of Nature and Science, 2001 Colorado Blvd., Denver, CO 80205*
[2]*Universidad Nacional Autónoma de México, Instituto de Biología, Mexico City*
    ✉ *edmundo.gonzalez@ib.unam.mx;* 🔾 *https://orcid.org/0000-0003-1340-068X*
*Corresponding author: ✉ *Paula.Cushing@dmns.org;* 🔾 *https://orcid.org/0000-0002-3423-7626*

Abstract

A new species in the unusual myrmecophagous family Myrmecicultoridae is described. This new species, *Myrmecicultor pueblaensis* **sp. nov.** shares several unique morphological features with the one other species in the family, *M. chihuahuensis* Ramírez, Grismado, and Ubick 2019. A multi-locus phylogenetic analysis of six molecular markers from the mitochondrial (12 S rDNA, 16S rDNA, cytochrome oxidase subunit I) and nuclear (18S rDNA, 28S rDNA, histone H3) genomes also places this new species as sister to *M. chihuahuensis*. In addition, the new species is a myrmecophage and shows similar hunting behavior to *M. chihuahuensis*. We hypothesize that additional species of this unusual family may be distributed throughout the desert ecosystems of southern Mexico in association with various species of ants.

Key words: Taxonomy, phylogenetics, morphology, ant symbiosis

Introduction

The spider family Myrmecicultoridae was established in 2019 by Ramírez *et al.* (2019). Until now it included a single species, *Myrmecicultor chihuahuensis* Ramírez, Grismado, and Ubick. Phylogenetic analysis based on mitochondrial and nuclear loci placed this family as a separate lineage emerging near the base of the Dinonycha and Oval Calamistrum clade. Myrmecicultoridae (and its monotypic species) is characterized by the following: two tarsal claws without claw tufts; procurved eye rows with the posterior median eyes (PME) oblong and with noticeable tapeta; the presence of a retrolateral tibial apophysis (RTA) on the male pedipalp; long fangs; a dorsal patch of setae on the palpal cymbium of males and on the pedipalp of females; a high clypeus; and a serrula on the endites of males and females. Subsequent research exploring the natural history and biology of this monotypic species determined that these spiders are myrmecophages (Cushing *et al.* 2022), hunting ants in a manner similar to that documented for spiders in the family Zodariidae (Pekár 2002; Cushing & Santangelo 2002).

From 8 – 9 July 2024, the authors were leading a field expedition to the desert habitat of the southern Mexican state of Puebla. While headlamping at night, each of the authors noticed groups of adult and juvenile spiders actively hunting on two different trails. This collective activity was so unusual that both authors independently collected multiple spiders (adults and immatures). Ants were also seen on the trails in the vicinity of these spiders. The first author (PEC) watched as one of the spiders approached an ant from behind, rushed forward, bit the rear leg of the ant, retreated, and waited for the venom to take effect. This myrmecophagous hunting behavior was identical to that reported by Cushing *et al.* (2022) for *M. chihuahuensis*. It was further determined that this species had similar morphological characters mentioned above for *M. chihuahuensis*. The morphological resemblance to this previously described species but the evident difference in epigynal and palpal structures led the authors to suspect the existence of a second species in the family Myrmecicultoridae, which is herein described under the name *Myrmecicultor pueblaensis* **sp. nov.**.

Materials and Methods

Material used

A total of 12 spiders were collected in Mexico, state of Puebla, 10 Km west of Zapotitlán Salinas at 18.33510° N, 97.51850° W, 1587 m elev. These 12 specimens included two males, five females, and five juveniles. One juvenile was destructively sampled for molecular sequencing. One male is designated (below) as the holotype, one female paratype is designated as the allotype, and the remaining specimens collected at this site are designated as additional paratypes. The holotype is deposited in the arachnology collection at the Universidad Nacional Autónoma de México (UNAM) with unique identifier, UID, #CNAN-Ar011706; all paratypes are deposited in the arachnology collection at the Denver Museum of Nature and Science (DMNS). The female allotype is separated from the rest of the paratypes in a sub-vial. The paratypes at DMNS have been assigned the unique identifier DMNS ZA.46195 and the collecting data (provenance, date, collector) recorded in the Ecdysis database (https://ecdysis.org/index.php) and pushed out to other data portals such as GBIF (https://www.gbif.org/).

Molecular sequencing

To determine the phylogenetic position of *M. chihuahuensis*, Ramírez *et al.* (2019) used both morphological character analysis as well as multi-locus DNA sequencing. Therefore, to test the hypothesis, suggested by the morphological similarity, that the Puebla specimens represent a new species in the family Myrmecicultoridae, we sequenced the following loci (also used by Ramírez *et al.* 2019): 12S rDNA (12S), the 3' end of the 16S rDNA (16S), and cytochrome oxidase subunit I (COI) from the mitochondrial genome and 18S rDNA (18S), the D3 large subunit ribosomal RNA 28S rDNA (28S), and a variable fragment of the histone H3 (H3) protein-coding gene from the nuclear genome (Table 1).

**TABLE 1.** Primer sequences used in the molecular analysis and associated GenBank numbers.

Gene	Name	Sequence (5'-3')	GenBank#s	References
COI	LCO1490	GGTCAACAAATCATAAAGATATTGG	PV448916	Folmer *et al.* (1994)
	HCO2198	TAAACTTCAGGGTGACCAAAAATCA		Folmer *et al.* (1994)
12S rDNA	12S-ai-F	AAACTAGGATTAGATACCCTATTAT	PV492139	Köcher *et al.* (1989)
	12S-bi-R	AAGAGCGACGGGCGATGTGT		Köcher *et al.* (1989)
16S rDNA	16Sar	CGCCTGTTTATCAAAAACAT	PV492140	Simon *et al.* (1994)
	16Sbr	CTCCGGTTTGAACTCAGATCA		Simon *et al.* (1994)
18s rDNA	18S-1F	TACCTGGTTGATCCTGCCAGTAG	PV449816	Carranza *et al.* (1996)
	18S-5R	CTTGGCAAATGCTTTCGC		Carranza *et al.* (1996)
28s rDNA	28Sa	GACCCGTCTTGAAACACGGA	PV449817	Nunn *et al.* (1996)
	28Sbout	CCCACAGCGCCAGTTCTGCTTACC		Prendini *et al.* (2005)
H3	H3af	ATGGCTCGTACCAAGCAGACVGC	PV454979	Colgan *et al.* (1998)
	H3ar	ATATCCTTRGGCATRATRGTGAC		Colgan *et al.* (1998)

For the molecular analysis, we destructively sampled one juvenile of the new species for the molecular analysis using a standard Qiagen Blood and Tissue DNA Extraction Kit (Qiagen, Germany) according to the manufacturer's instructions in the Genomics Lab at the DMNS. Gene fragments were amplified using the polymerase chain reaction (PCR). For each locus, we used the protocol outlined in Cushing *et al.* (2015) or in Wheeler *et al.* (2017). All PCR mixes contained 15 μl DreamTaq, 10.1 μl nuclease-free water, 1.2 μl each of forward and reverse primers, and 2 μl of genomic DNA. Nuclease-free water was used as the negative control in each run. For all primer sets (see Table 1 for primer sequences), the PCR amplification protocol was 95°C for 4 min followed by 40 cycles of 95°C for 30 s,

49°C for 30 s and 72°C for 1 min plus a final extension step of 72°C for 3 min. The COI PCR product was sequenced in both directions at EtonBio (Durham, North Carolina, USA). All remaining loci were sequenced in both directions at Quintara Biosciences (Cambridge, Massachusetts, USA). Double-stranded sequences were assembled using the Geneious version 2024.0.2 program package. BLAST analysis was performed to compare the sequences with those in the NCBI GenBank. All sequences generated for this study were deposited in GenBank.

Phylogenetic analysis

We deconstructed the original matrix built by Ramírez *et al.* (2019) to incorporate our fresh samples. The loci were re-assembled using Mesquite 3.81 (Maddison and Maddison, 2023). The consensus sequences for individual loci were aligned in the online version of MAFFT (Katoh *et al.* 2019). The final data matrix comprised 6468 aligned bp with 50 terminals with 3191 distinct patterns, 2068 parsimony-informative, 885 singleton, and 3514 constant sites, after editing by eye. The phylogenetic relationships were reconstructed from the aligned data set with Maximum Likelihood (ML) as optimality criterion using IQ-TREE2 (version 2.4.0) software, in which ModelFinder automatically selected the appropriate molecular model for each partition (Kalyaanamoorthy *et al.* 2017) and calculated ultrafast bootstrap approximation (Hoang *et al.* 2018). Selected molecular model included: TIM2+F+I+G4: 12s; GTR+F+I+G4: 16s; TIM2e+I+G4: 18s; TIM3+F+I+G4: 28s; GTR+F+I+G4: COI; GTR+F+I+G4: COI_1; TIM+F+I+G4: COI_2; K3Pu+F+G4: COI_3; TPM2+I+G4: H3; GTR+F+G4: H3_1; JC+I: H3_2; SYM+G4: H3_3. For the protein coding genes COI and H3, the stop codons were minimized with Mesquite (Maddison & Maddison 2023).
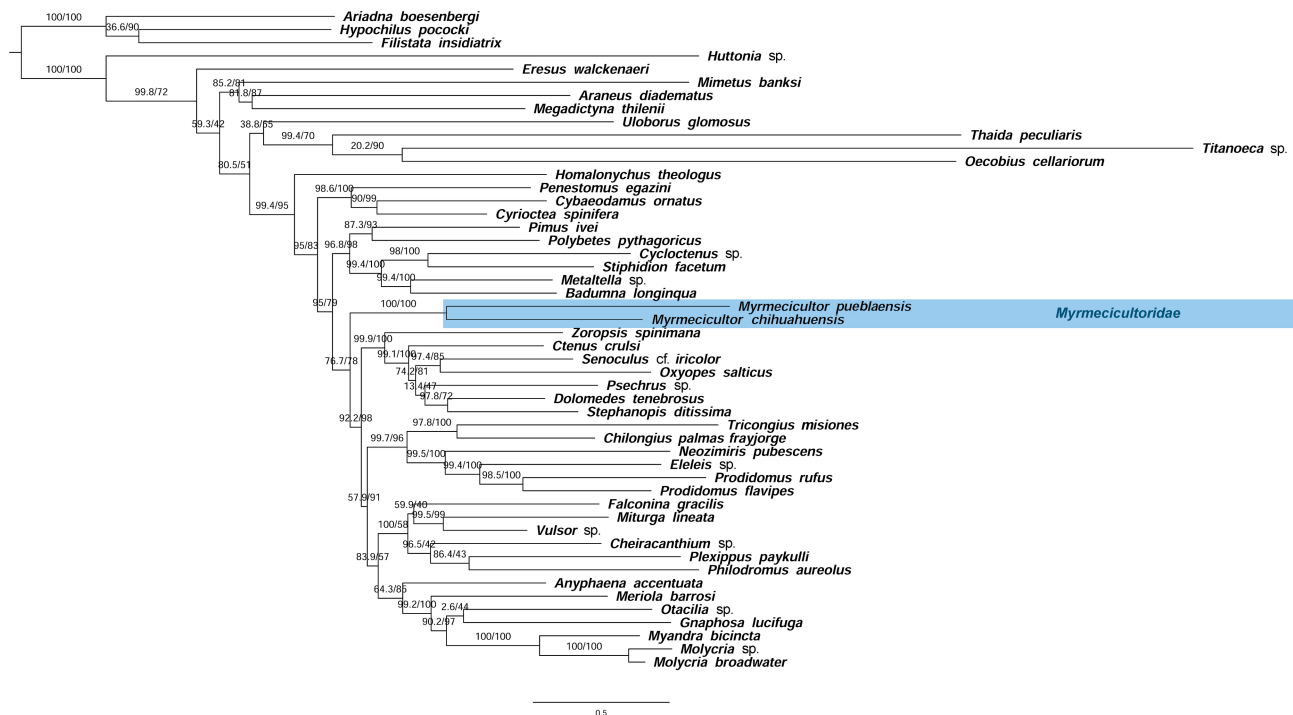
FIGURE 1. Phylogenetic tree resulting from the analysis of six genetic markers on the optimality criterion of ML best score - 88631.383. The blue box indicates the circumscription of the family Myrmecicultoridae with the known species *M. chihuahuensis* and *M. pueblaensis* **sp. nov.** The topology shown here is identical to that obtained by Ramirez *et al.* (2019). Branch support on the tree indicates SH-like aLRT/Ultrafast bootstrap values.

Imaging

We used a Keyence VHS high resolution digital imaging system with proprietary stacking software to compare the morphology of *M. chihuahuensis* with the new species. Because the molecular phylogenetic analysis clearly placed the new species in a clade with *M. chihuahuensis* and because we had limited adult specimens to work with (2 males and 5 females), we did not review the complete dataset of 397 morphological characters used in

Ramírez *et al.* (2019); rather, we focused on assessing and imaging characters that could be seen under light microscopy and that were either unique to the family Myrmecicultoridae when compared to other members of the same phylogenetic clade (see Ramirez *et al.* 2019, fig. 2A) or distinct for this newly discovered species. In the parsimony analysis of morphological data included in Ramírez *et al.* (2019, fig. 2 A), Myrmecicultoridae shared a clade with Homalonychidae (*Homalonychus theologus* Chamberlin 1924) and with two species of Zodariidae (*Cybaeodamus ornatus* Mello-Leitão 1938 and *Cyrioctea spinifera* (Nicolet 1849)). Morphological characters assessed and compared between the two species of the genus *Myrmecicultor* are listed in Table 2.

TABLE 2. Morphological characters assessed for the new species and comparison with *Myrmecicultor chihuahuensis*. AME = Anterior Median Eye; PME = Posterior Median Eye. See Ramírez 2014 for descriptions of these characters.

Character	*M. chihuahuensis*	*Myrmecicultor pueblaensis* sp. nov.
Clypeus	High	High
Anterior eye row curvature in anterior view	Notably procurved	Notably procurved
Posterior eye row curvature in dorsal view	Notably procurved	Notably procurved
ALE black cup	Eye with silvery tapetum on top of the dark background	Eye with silvery tapetum on top of the dark background; ALE only partly surrounded by black pigment.
Eyes surrounded by black pigment	Eyes mostly surrounded by black pigment	Eyes mostly surrounded by black pigment
PME lens curvature	Convex	Flattened
PME tapeta symmetry axes	Orthogonal to each other	Orthogonal to each other
Fovea	Dark, longitudinal	Dark, longitudinal
Carapace shape	Highest in cephalic region	Highest in cephalic region
Cheliceral boss	Absent	Absent
Cheliceral promarginal teeth	One small tooth	No teeth
Cheliceral retromarginal teeth	No teeth	One retromarginal tooth and proximal denticle (diastema between)
Fang length	Very long with shaft serrula	Short with shaft serrula
Labium length/width ratio	Wider than long	Wider than long
Endites obliquely depressed	Not depressed	Depressed
Endite ventral distal macrosetae	Absent	Present
Endite shape	As wide as long	Longer than wide
Serrula on endites	Present	Present
Serrula rows	Single row	Single row
Serrula width	Wide, bordering apex	Wide, bordering apex
Female palpal tarsus dorsal chemosensory setae distribution	In a defined patch	In a defined patch
Male palpal tarsus dorsal chemosensory setae distribution	In a defined patch	In a defined patch
Palpal claw teeth	Many teeth in a row	Many teeth in a row
Sternum posterior end profile	Convex	Convex
Sternum shape	Heart shaped	Shield shaped
Pointed extension sternum between coxae IV	Yes	Yes
Precoxal triangles in female	Absent	Present, fused to sternum
Trochanter IV length	Less than 1.5 X length of trochanter III	Less than 1.5 X length of trochanter III for males; greater than for females
Preening brush	Legs III & IV	Legs III & IV (less developed on LIV)

CUSHING & GONZÁLEZ SANTILLÁN

TABLE 2. (Continued)

Character	*M. chihuahuensis*	*Myrmecicultor pueblaensis* sp. nov.
RTA position	Medial	Apical
RTA with canal	Present	Present
Cymbium dorsal chemosensory patch	Present	Present
Prey-catching web	Absent	Absent
Wrap-bite attack	Bite first	Bite first
Orb web architecture	NA	NA
Ant hunting behavior	Present	Present
Ant shielding behavior	Present	Unknown

Abbreviations

Abbreviations used in the taxonomic section include: AER, Anterior Eye Row; ALE, Anterior Lateral Eye; PER, Posterior Eye Row; PME, Posterior Median Eye; and RTA, Retrolateral Tibial Apophysis (of the palp). Roman numerals are used to designate legs from anterior to posterior (I, II, III, IV) or leg segments from proximal to distal (ibid).

Results

The analysis of the sequence data placed this new species as sister to *M. chihuahuensis* in the family Myrmecicultoridae with strong branch support (Fig. 1). The morphological characters the new species shares with *M. chihuahuensis* include the following (Table 2 and Figs. 2-6): a noticeably high clypeus (Figs. 3A, B); a narrow, dark longitudinal fovea (Figs. 2A - D); procurved AER and PER (Figs. 2 & 3); ALE with silvery tapetum on top of a dark cup (Fig. 3); PME tapeta orthogonal to each other (Figs. 2A - D); similarly shaped sternum in both species with pointed extensions between coxae IV (Figs. 2 E, F; although the anterior sternal plate of the new species is more rounded); no cheliceral boss; labium wider than long; presence of a serrula on the anterior apex of the endites of males and females (Fig. 6A, white arrows); a distinct patch of setae on the male dorsoapical cymbium and female palpal tarsus (Figs. 5G, 5H, 6C); two tarsal claws without claw tufts; female palpal claws with many teeth in a row; six reduced, tightly grouped spinnerets (Fig. 6B); metatarsi III & IV with a preening brush; males with a RTA (Figs. 5G, H); and a well-developed female palpal claw. In addition, both species are myrmecophages with similar hunting strategies.

Taxonomy

Myrmecicultor pueblaensis Cushing and González-Santillán, sp. nov.
Figures 2B, 2D, 2F, 3B, 4B, 4D, 4F, 5D, 5E, 5F, 5H, 6

Type series. Male holotype (UNAM CNAN-Ar011706); female allotype and additional paratypes (DMNS ZA.46195). All specimens collected in Mexico, Puebla, 10 Km west of Zapotitlán Salinas, N 18.33510°, W 97.51850°, 1587 m elev.; 9 July 2024; collected by authors while headlamping at night from 20:00 – 23:30 hrs. This desert habitat is within the Poblano-Oaxaca Semiarid Region (Abd El-Ghani *et al.* 2017).

Etymology. The specific epithet is an adjective referring to the state of Puebla, Mexico. This is, thus far, the only locality from which these spiders have been collected.

Diagnosis. The two species of *Myrmecicultor* differ in the following morphological characters (Table 2, Figs. 2–5): PME lens convex in *M. chihuahuensis* and flattened in *M. pueblaensis* **sp. nov.**; cheliceral basal transverse ridge is absent in *M. chihuahuensis* and present in *M. pueblaensis* **sp. nov.**; cheliceral promargin teeth are present in *M. chihuahuensis* and absent in *M. pueblaensis* **sp. nov.**; pronounced mound on the cheliceral retromargin is absent in *M. chihuahensis* and present in *M. pueblaensis* **sp. nov.**; the endites are not obliquely depressed in
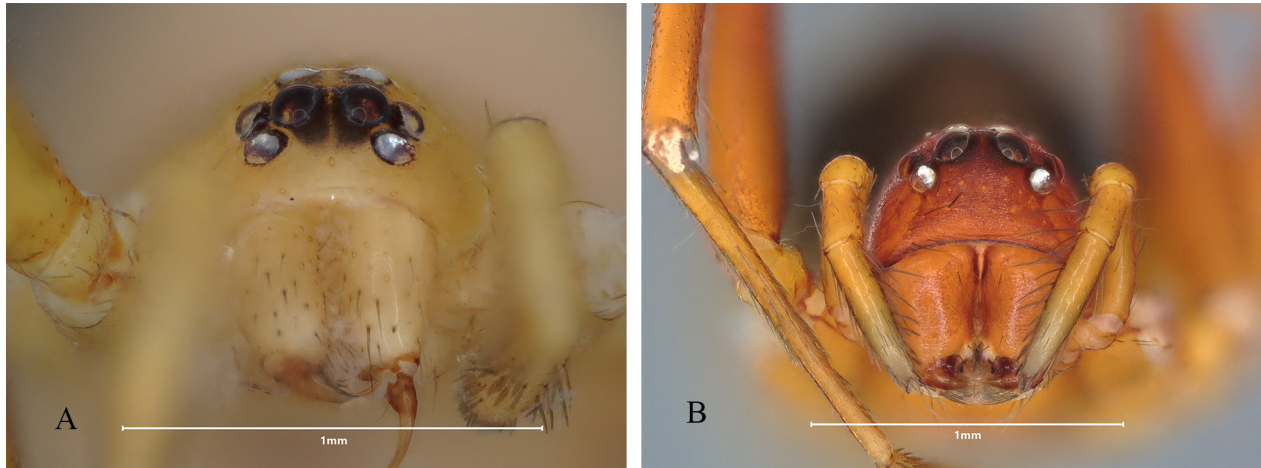
M. chihuahuensis but are so in *M. pueblaensis* **sp. nov.** and the endites are only slightly longer than wide in *M. chihuahuensis* (more or less triangular in shape) whereas the endites of *M. pueblaensis* **sp. nov.** are distinctly longer than wide (compare Figs. 2 E and F); ventral distal macrosetae on the endites are absent in *M. chihuahuensis* whereas *M. pueblaensis* **sp. nov.** has a scattering of ventral distal macrosetae; the anterior margin of the sternum is straight in *M. chihuahuensis* and convex in *M. pueblaensis* **sp. nov.** (compare Figs. 2E and F); precoxal triangles on the female are absent in *M. chihuahuensis* and present (fused to the sternum) in *M. pueblaensis* **sp. nov.** (Figs. 2 E and F).

FIGURE 2. Dorsal habitus of *Myrmecicultor chihuahuensis* and *M. pueblaensis* **sp. nov.** and ventral views of promsoma. A) Habitus, female *M. chihuahuensis* (DMNS ZA.41786); B) Habitus, female *M. pueblaensis* **sp. nov.**; C) Habitus, male *M. chihuahuensis* (DMNS ZA.41786); D) habitus, male *M. pueblaensis* **sp. nov.**; E) *M. chihuahuensis* female sternum (DMNS ZA.44217); F) *M. pueblaensis* **sp. nov.** female sternum. Scale bars = 1 mm.

In addition, *M. chihuahuensis* has a broader and more medially positioned RTA in *M. chihuahuensis* whereas the RTA is more more elongate and more apically positioned in *M. pueblaensis* **sp. nov.** (Figs. 5G, H). The dorsal color pattern of the two species are also distinctive: *M. chihuahuensis* has a pale yellow carapace and pale abdomen lacking patterns; *M. pueblaensis* **sp. nov.** has a dark brownish-orange carapace and the abdomen is dark grey with three distinct white markings (Figs. 2 A-D). The fangs of *M. chihuahuensis* are long and thin whereas *M. pueblaensis* **sp. nov.** has much shorter fangs.

FIGURE 3. Anterior views of *Myrmecicultor chihuahuensis* and *M. pueblaensis* **sp. nov.** females (male aspects are similar to females for both species). A) Anterior view of *M. chihuahuensis* female showing the high clypeus and the procurved AME (DMNS ZA.44217); B) Anterior view of *M. pueblaensis* **sp. nov.** female.

Description. Ecribellate entelegyne spider with two tarsal claws, lacking claw tufts; males with RTA (Fig. 5H); with six spinnerets in a tight group (Fig. 6B); female palpal claw well developed with several teeth in a row; AME and PME recurved (Figs. 2B, 2D, 3 B); PME oblong, oval with well-developed obliquely oriented tapeta (Figs. 2B, D); serrula on anterior border of endites (arrow Fig. 6A); endites elongate and medially depressed; dorsal apical patch of setae on cymbium of males (Fig. 5H) and palp of females (Fig. 6C); and distinct, precoxal triangles fused to sternum (Fig. 2F). Chelicerae with one retromarginal tooth and denticle with large diastema between; promargin with no teeth; lightly sclerotized area beside three large bristle-setae on promargin (Fig. 6A); short fangs with serrated edge; serrula on edge of endites (Fig. 6A, white arrow); anterior part of fangs translucent with venom duct evident (Fig. 6A). Genitalia as illustrated in Figs. 4 and 5.

Male holotype (UNAM CNAN-Ar011706): All measurements in mm. Total length 2.47. Carapace broadly oval in dorsal view, highest in front of fovea. Carapace length 1.06; width 1.00. Clypeus high, almost twice ALE diameter. Clypeus height at AME 0.19; at ALE 0.17. Fovea a narrow, dark longitudinal line. Carapace highest in cephalic region. Sternum shield-shaped with pointed extension between coxae IV. Precoxal triangles faint but present. Marginal setae on sternum. Labium length 0.12; width 0.23. Endite length 0.4; width 0.19. Serrula on anterior margin of endites. Eyes: AME diameter 0.10, ALE diameter 0.10, PME diameter 0.09, PME length 0.11, PLE diameter 0.09. Eye inter-distances: AME-AME 0.07, AME-PME 0.05, AME-ALE 0.02, PME-PME 0.03, PME-PLE 0.08, ALE-PLE 0.04. AER 0.41. PER 0.48. Eyes ringed with black pigment; tapeta present in PME, PLE, and ALE. Leg I total 4.81 (femur 1.35, patella 0.40, tibia 1.16, metatarsus 1.19, tarsus 0.71). Leg II total 4.22 (femur 1.18, patella 0.38, tibia 1.00, metatarsus 1.04, tarsus 0.62). Leg III total 4.19 (femur 1.24, patella 0.38, tibia 0.87, metatarsus 1.10, tarsus 0.60). Leg IV total 5.65 (femur 1.62, patella 0.40, tibia 1.35, metatarsus 1.50, tarsus 0.78). Leg formula IV, I, II, III. Color: dorsal abdomen with two anterior large white dots and posterior white mark consisting partly of white flattened setae surrounded by dark greyish-black background (Fig. 2D). Additional flat white setae scattered on dorsum; ventral abdomen white; legs orange with femora slightly darker; carapace orange with scattered white setae, particularly on cephalon. All legs with single spine on proximal-dorsal surface of femora; no ventral spines. All legs with flattened, translucent setae on dorsum of femora. Metatarsi III & IV with preening brush (Fig. 6D). Thick, comb-like setae on all tarsi. Single trichobothria on distal dorsal metatarsi; several trichobothria on tarsi. Trochanter IV 1.3 times trochanter III. Palp as in Figs. 5D, E, F, H. Cymbium with dorsoapical patch of sensory setae (Fig. 5H). Conductor bifurcate at tip (Fig. 5D and embolus tube distinctly visible at tip (Fig. 5F).

FIGURE 4. Comparison of female genitalia of *M. chihuahuensis* (DMNS ZA.44217) and *M. pueblaensis* **sp. nov.** A) Female epigynum of *M. chihuahuensis*; B) Female epigynum of *M. pueblaensis* **sp. nov.**; C) Cleared dorsal epigynal structures of *M. chihuahuensis*; D) Cleared dorsal epigynal structures of *M. pueblaensis* **sp. nov.**; E) cleared ventral epigynal structures of *M. chihuahuensis*; F) cleared ventral epigynal structures of *M. pueblaensis* **sp. nov.** Scale bars = 500 μm.

FIGURE 5. Comparison of left palps of males. All views for *M. chihuahuensis* are of paratype DMNS ZA.41786; views for *M. pueblaensis* **sp. nov.** are of the holotype. A) Ventral view of *M. chihuahuensis*; B) Prolateral view of *M. chihuahuensis*; C) Retrolateral view of *M. chihuahuensis*; D) Ventral view male palp of *M. pueblaensis* **sp. nov.**; E) Prolateral view of *M. pueblaensis* **sp. nov.**; F) Retrolateral view of *M. pueblaensis* **sp. nov.**; G) RTA of *M. chihuahuensis* with distal setal patch visible (arrow); H) RTA of *M. pueblaensis* **sp. nov.** palpal tarsus with distal setal patch visible (arrow). Scale bars = 500 µm; Co = conductor; Em = embolus.

FIGURE 6. Additional diagnostic morphology of *M. pueblaensis* **sp. nov.** Female paratype (DMNS ZA.46195). A) Dorsal view of chelicerae, white arrow points to serrula visible on anterior edge of endites; B) Spinnerets; C) Patch of palpal setae on female pedipalp. Scale bars = 500 μm for A-C. D) Preening brush of Leg III, scale bar = 1 mm.

Female allotype (DMNS ZA.46195; largest female in lot, separated from other paratypes): Total length 3.68. Carapace length 1.5; width 1.29. Clypeus at AME 0.30; at ALE 0.21. Fovea a narrow, dark longitudinal line. Carapace highest in cephalic region. Sternum shield-shaped with pointed extension between coxae IV. Precoxal triangles distinct (Fig. 2F). Marginal setae on sternum. Labium length 0.18; width 0.28. Endite length 0.55; width 0.19. Serrula on anterior margin of endites. Eyes: AME diameter 0.13, ALE diameter 0.12, PME diameter 0.10, PME length 0.13, PLE diameter 0.09. Eye inter-distances: AME-AME 0.10, AME-PME 0.09, AME-ALE 0.03, PME-PME 0.06, PME-PLE 0.12, ALE-PLE 0.05. AER 0.50. PER 0.60. Tapeta present in PME, PLE, and ALE. Leg I total 5.87 (femur 1.59, patella 0.51, tibia 1.32, metatarsus 1.55, tarsus 0.90). Leg II total 5.26 (femur 1.46, patella 0.51, tibia 1.10, metatarsus 1.44, tarsus 0.75). Leg III total 5.09 (femur 1.37, patella 0.51, tibia 1.03, metatarsus 1.51, tarsus 0.67). Leg IV total 6.74 (femur 1.92, patella 0.52, tibia 1.60, metatarsus 1.88, tarsus 0.82). Leg formula IV,I,II,III. Color: dorsal abdomen with two anterior large white dots and posterior white mark consisting partly of white flattened setae surrounded by dark greyish-black background (Fig. 2B). Additional flat white setae scattered on dorsum; ventral abdomen white; legs orange with femora slightly darker; carapace orange with scattered white setae, particularly on cephalon. All legs with single spine on proximal-dorsal surface of femora; no ventral spines. All legs with flattened, translucent setae on dorsum of femora. Metatarsi III & IV with preening brush, although brush on IV is reduced. Thick, comb-like setae on all tarsi. Single trichobothria on distal dorsal metatarsi; several trichobothria on tarsi. Trochanter IV 1.94 times trochanter III. Female ventral and dorsal epigynal structures as in Figs. 4B, D, F: two small copulatory openings lead internally to copulatory tubes. Spermathecae widely separated (Figs. 4D, F).

Male paratype (DMNS ZA.46195; male placed in vial with female paratypes described below): Color, markings, setal characters, body shape, leg formula as for the holotype except leg femora not noticeably darker and pre-coxal triangles present but faint. Measurements as follows. Total length 2.56. Carapace length 1.17; width 0.98. Clypeus at AME 0.24; at ALE 0.16. Labium length 0.14; width 0.23. Endite length 0.39; width 0.15. Eyes: AME diameter 0.09, ALE diameter 0.09, PME diameter 0.10, PME length 0.11, PLE diameter 0.09. Eye inter-distances: AME-AME 0.09, AME-PME 0.04, AME-ALE 0.03, PME-PME 0.04, PME-PLE 0.10, ALE-PLE 0.02. AER 0.41. PER 0.48. Leg I total 4.93 (femur 1.40, patella 0.40, tibia 1.17, metatarsus 1.25, tarsus 0.71). Leg II total 4.19 (femur 1.12, patella 0.38, tibia 0.94, metatarsus 1.11, tarsus 0.64). Leg III 4.14 (femur 1.11, patella 0.39, tibia 0.83, metatarsus 1.19, tarsus 0.62). Leg IV total 5.47 (femur 1.56, patella 0.41, tibia 1.30, metatarsus 1.50, tarsus 0.70).

Female paratypes (DMNS ZA.46195, 4 females placed in with male paratype): Color, markings, setal characters, body shape, leg formula as for allotype except one female has both marginal setae on sternum as well as scattered setae on center area of sternum. Measurements as follows. Total lengths: 3.75, 3.20, 2.97, 2.87 (all females, $\bar{x}$ including allotype = 3.29). Carapace lengths: 1.34, 1.32, 1.32, 1.39 (all females, $\bar{x}$ = 1.37). Carapace widths: 1.22, 1.16, 1.10, 1.20 (all females, $\bar{x}$ = 1.19). Clypeus at AME: 0.32, 0.25, 0.25, 0.27 (all females, $\bar{x}$ = 0.28). Clypeus at ALE: 0.24, 0.17, 0.17, 0.20 (all females, $\bar{x}$ = 0.20). Labium lengths: 0.17, 0.17, 0.13, 0.17 (all females, $\bar{x}$ = 0.16). Labium widths: 0.29, 0.26, 0.32, 0.28 (all females, $\bar{x}$ = 0.29). Endite lengths: 0.44, 0.44, 0.49, 0.41 (all females, $\bar{x}$ = 0.47). Endite widths: 0.20, 0.19, 0.21, 0.20 (all females, $\bar{x}$ = 0.20). AME diameters: 0.13, 0.10, 0.10, 0.10 (all females, $\bar{x}$ = 0.11). ALE diameters: 0.10, 0.10, 0.11, 0.11 (all females, $\bar{x}$ = 0.11). PME diameters: 0.10, 0.10, 0.11, 0.08 (all females, $\bar{x}$ = 0.10). PME lengths: 0.15, 0.12, 0.13, 0.13 (all females, $\bar{x}$ = 0.13). PLE diameters: 0.11, 0.08, 0.10, 0.10 (all females, $\bar{x}$ = 0.10). AME-AME: 0.10, 0.08, 0.10, 0.10 (all females, $\bar{x}$ = 0.10). AME-PME: 0.07, 0.07, 0.09, 0.07 (all females, $\bar{x}$ = 0.08). AME-ALE: 0.04, 0.04, 0.03, 0.03 (all females, $\bar{x}$ = 0.03). PME-PME: 0.03, 0.03, 0.03, 0.05 (all females, $\bar{x}$ = 0.04). PME-PLE: 0.13, 0.12, 0.13, 0.11 (all females, $\bar{x}$ = 0.12). ALE-PLE: 0.06, 0.05, 0.04, 0.05 (all females, $\bar{x}$ = 0.05). AER: 0.59, 0.47, 0.48, 0.49 (all females, $\bar{x}$ = 0.51). PER: 0.59, 0.53, 0.52, 0.54 (all females, $\bar{x}$ = 0.56). Leg I totals: 5.51, 5.18, 4.98, 5.39 (all females, $\bar{x}$ = 5.39). Leg II totals: 4.86, 4.55, 4.55, 4.72 (all females, $\bar{x}$ = 4.79). Leg III totals: 4.77, 4.50, 4.40, 4.56 (all females, $\bar{x}$ = 4.66). Leg IV totals: 6.19, 5.75, 5.86, 6.03 (all females, $\bar{x}$ = 6.11).

Natural History: Spiders observed hunting in large groups made up of adult males, females, and juveniles in open areas of desert habitat. Ants seen in the vicinity with the spiders. Ants not collected or identified. One spider observed approaching ant from behind, biting rear leg, then retreating. This hunting behavior is essentially identical to the myrmecophagous behavior observed for *M. chihuahuensis* (Cushing *et al.* 2022). We suspect that the genus *Myrmecicultor* may be found throughout the desert habitats of southern Mexico and that additional species may be found in association with various species of ants as has been documented for *M. chihuahuensis* (Ramírez *et al.* 2019; Cushing *et al.* 2024).

Data Availability Statement

Acknowledgements

References

Abd El-Ghani, M.M., Huerta-Martínez, F.M., Hongyan, L. & Qureshi, R. (2017) The Deserts of Mexico. *In*: *Plant Responses to Hyperarid Desert Environments*. Springer, Cham, pp. 473–501.
https://doi.org/10.1007/978-3-319-59135-3_9

Carranza, S., Giribet, G., Ribera, C., Baguña, J. & Riutort, M. (1996) Evidence that two types of 18S rDNA coexist in the genome of *Dugesia (Schmidtea) mediterranea* (Platyhelminthes, Turbellaria, Tricladida). *Molecular Biology and Evolution*, 13 (6), 824–832.
https://doi.org/10.1093/oxfordjournals.molbev.a025643

Colgan, D.J., McLauchlan, A., Wilson, G.D.F., Livingston, S.P., Edgecombe, G.D., Macaranas, J., Cassis, G. & Gray, M.R. (1998) Histone H3 and U2 snRNA DNA sequences and arthropod molecular evolution. *Australian Journal of Zoology*, 46, 419–437.
https://doi.org/10.1071/ZO98048

Cushing, P.E., Brückner, A., Rogers, J.W. & Horner, N.V. (2022) Trophic specialization of a newly described ant symbiont, *Myrmecicultor chihuahuensis* (Araneae: Myrmecicultoridae). *Journal of Arachnology*, 50, 250–255.
https://doi.org/10.1636/JoA-S-21-072

Cushing, P.E., Graham, M.R., Prendini, L. & Brookhart, J.O. (2015) A multilocus molecular phylogeny of the endemic North American camel spider family Eremobatidae (Arachnida: Solifugae). *Molecular Phylogenetics and Evolution*, 92, 280–293.
https://doi.org/10.1016/j.ympev.2015.07.001

Cushing, P.E. & Santangelo, R.G. (2002) Notes on the natural history and hunting behavior of an ant eating zodariid spider (Arachnida, Araneae) in Colorado. *Journal of Arachnology*, 30 (3), 618–621.
https://doi.org/10.1636/0161-8202(2002)030[0618:NOTNHA]2.0.CO;2

Cushing, P.E., Wicker, R.M. & Horner, N.V. (2024) Living with the enemy: behavioral study of *Myrmecicultor chihuahuensis* Ramírez, Grismadeo & Ubick (Araneae: Myrmecicultoridae). *Journal of Arachnology*, 52, 71–74.
https://doi.org/10.1636/JoA-S-22-063

Folmer, O., Black, M.B., Hoch, W., Lutz, R.A. & Vrijehock, R.C. (1994) DNA primers for amplification of mitochondrial Cytochrome c Oxidase subunit I from diverse metazoan invertebrates. *Molecular Marine Biology and Biotechnology*, 3, 294–299.

González-Santillán, E. (2025) Matrix, partition and tree for the publication "A new species in the spider family Myrmecicultoridae and evidence of myrmecophagy in the family". Versión 1. *Zenodo*. [published online]
https://doi.org/10.5281/zenodo.15164897

Hoang, D.T., Chernomor, O., von Haeseler, A., Minh, B.Q. & Vinh, L.S. (2018) UFBoot2: Improving the ultrafast bootstrap approximation. *Molecular Biology and Evolution*, 35, 518–522.
https://doi.org/10.1093/molbev/msx281

Kalyaanamoorthy, S., Minh, B.Q., Wong, T.K.F., von Haeseler, A. & Jermiin, L.S. (2017) ModelFinder: Fast model selection for accurate phylogenetic estimates. *Nature Methods*, 14, 587–589.
https://doi.org/10.1038/nmeth.4285

Katoh, K., Rozewicki, J. & Yamada, K.D. (2019) MAFFT online service: multiple sequence alignment, interactive sequence choice and visualization. *Briefings in Bioinformatics*, 4, 1160–1166.
https://doi.org/10.1093/bib/bbx108

Köcher, T.D., Thomas, W.K., Meyer, A., Edwards, S.V., Pääbo, S., Villablanca, F.X. & Wilson, A.C. (1989) Dynamics of mitochondrial DNA evolution in animals: amplification and sequencing with conserved primers. *Proceedings of the National Academy of Sciences*, 86 (16), 6196–6200.
https://doi.org/10.1073/pnas.86.16.6196

Maddison, W.P. & Maddison, D.R. (2023) Mesquite: a modular system for evolutionary analysis. Version 3.81. Available from: https://www.mesquiteproject.org (accessed 4 November 2025)

Nunn, G.B., Theisen, B.F., Christensen, B. & Arctander, P. (1996) Simplicity-correlated size growth of the nuclear 28S ribosomal RNA D3 expansion segment in the crustacean order Isopoda. *Journal of Molecular Evolution*, 42, 211–223.
https://doi.org/10.1007/BF02198847

Pekár, S. (2002) Revision of the genus *Zodarion* (Araneae: Zodariidae) in the Czech and Slovak Republics. *Acta Societatis Zoologicae Bohemicae*, 66, 51–66.

Prendini, L., Weygoldt, P. & Wheeler, W.C. (2005) Systematics of the *Damon variegatus* group of African whip spiders (Chelicerata: Amblypygi): evidence from behaviour, morphology and DNA. *Organisms, Diversity and Evolution*, 5, 203–236.
https://doi.org/10.1016/j.ode.2004.12.004

Ramírez, M.J. (2014) The morphology and phylogeny of Dionychan spiders (Araneae: Araneomorphae). *Bulletin of the American Museum of Natural History*, 390, 1–374.
https://doi.org/10.1206/821.1

Ramírez, M.J., Grismado, C.J., Ubick, D., Ovtsharenko, V., Cushing, P.E., Platnick, N.I., Wheeler, W.C., Prendini, L., Crowley, L.M. & Horner, N.V. (2019) Myrmecicultoridae, a new family of myrmecophilc spiders from the Chihuahuan Desert

(Araneae: Entelegynae). *American Museum Novitates*, 3930, 1–24.
https://doi.org/10.1206/3930.1

Simon, C., Frati, F., Beckenback, A., Crespi, B., Liu, H. & Flook, P. (1994) Evolution, weighting, and phylogenetic utility of mitochondrial gene sequences and a compilation of conserved polymerase chain reaction primers. *Annals of the Entomological Society of America*, 89, 641–701.
https://doi.org/10.1093/aesa/87.6.651

Wheeler, W.C., Coddington, J.A., Crowley, L.M., Dimitrov, D., Goloboff, P.A., Griswold, C.E., Hormiga, G., Prendini, L., Ramírez, M.J., Sierwald, P., Almeida-Silva, L., Alvarez-Padilla, F., Arnedo, M.A., Benavides Silva, L.R., Benjamin, S.P., Bond, J.E., Grismado, C.J., Hasan, E., Hedin, M., Izquierdo, M.A., Labarque, F.M., Ledford, J., Lopardo, L., Maddison, W.P., Miller, J.A., Piacentini, L.N., Platnick, N.I., Polotow, D., Silva-Dávila, D., Scharff, N., Szűts, T., Ubick, D., Vink, C.J., Wood, H.M. & Zhang, J. (2017) The spider tree of life: phylogeny of Araneae based on target-gene analyses from an extensive taxon sampling. *Cladistics*, 33, 574–616.
https://doi.org/10.1111/cla.12182